18th International Conference on Renewable Energies and Power Quality (ICREPQ'20)
Granada (Spain), 1st to 2nd April 2020
Renewable Energy and Power Quality Journal (RE&PQJ)
ISSN 2172-038 X, Volume No.18, June 2020

Simulink model of a bifacial PV module based on the manufacturer datasheet

S. Vergura

Department of Electrical and information Engineering
Polytechnic University of Bari
st. E. Orabona, 4, 70125, Bari, ITALY
Phone:+0039 080 5963590, e-mail: silvano.vergura@poliba.it

Abstract. The paper proposes an update of a mathematical model of a Photo-Voltaic (PV) module, considering the possibility that also the rear face of the PV module produces energy. The proposed approach allows to write a new descriptive equation, whose terms are function of the information always available in the modern datasheet of the PV module's manufacturers. This implies that no pre-processing of the datasheet's parameters is needed to use the proposed model, whichever are the solar irradiance and the cell/module temperature. The model considers the total solar radiation (front and back side), such that the produced energy increases. Simulink environment is used to calculate the total solar radiation.

Keywords
PV module model, bifacial module, I-V curve, datasheet's parameters, variable environment condition, Simulink.

1. Introduction

The energy performance of a PV system depends on many environment parameters, nevertheless two of them are mainly responsible: the solar irradiance and the cell temperature. The former strongly affects the short-circuit current, the latter the open-circuit voltage; both affect the Maximum Power Point (MPP). Therefore, a reliable model of a PV system must take into account these parameters for any typology of investigation: monitoring of the performance [1], forecasting of the produced power [2], development and testing of maximum power point tracking algorithms [3], and so on. A reliable model is also needed to study the defected PV cell [4]. In these cases, the thermal issues are relevant to classify the size and the severity of the defects, as described in [5-7].
There exist also several equivalent circuits based on a photocurrent source, one or more resistors, and one or more diodes. These topologies are characterized by several unknowns to be calculated; in fact, the models are also classified with respect to the total number of unknowns. For example, the widely used *single-diode* model is also known as *five-parameters* model, because it may be completely characterized by five parameters, as it will be seen later. Instead, the *double-diode* model is known as the *seven-parameters* model, because two additional parameters must be calculated, other than those of the *five-parameters* model. Both previous models are based on the accuracy through three characteristic points of the current-voltage (I-V) curve (open-circuit condition, short-circuit condition, and MPP) [8], and they are based on a mono-facial PV module, i.e. a module that captures the solar radiation only on a front surface.
The drawback of many models is that the values of the components (resistors, diodes, etc.) are not reported in any manufacturer's datasheet. Instead, the datasheets contain electrical information and some temperature-dependent coefficients. Thus, it needs almost always a pre-processing of the values reported into the datasheet before using the five- or seven-parameters model. Several authors are investigating this issue and there already exist PV models that consider these issues [9-11], even if only for a mono-facial PV module.
Bifacial modules are characterized by their ability to collect light on the PV cells located on the front side, as well as on the PV cells located on the rear side. In this way, a surplus of energy is produced by a bi-facial PV module with respect to a mono-facial PV module constituted by the same PV cells, in the same environmental conditions. Moreover, the energy produced by bifacial PV modules relative to monofacial designs depends strongly on the deployment scenario. In any case, the researchers have already demonstrated that additional energy gain of 5%–25% are possible under several ground-cover scenarios and mounting configurations [12,13]. The collection of the rear irradiation is based on the diffuse and ground-reflected energy, therefore uncertainty exists about the expected performance for individual system configurations.
In fact, back surface irradiance is a result of illumination and system parameters. Illumination depends on the geographical location's conditions due to sun position, direct and diffuse radiation components, and climate. Installation conditions must consider row-to-row distance, clearance from the ground, tilt, and the albedo of the underlying surface [14]. Another effect regards the presence or not of tracking systems. For example, some reserachers have compared the model results against field performance data for two side-by-side bifacial and monofacial tracked systems: the first one located in Albuquerque, USA, and the other one located in eastern Oregon. While, the first PV system showed a monthly rear irradiance gain of 10%–14.9%, the second showed an average performance ratio 9.4% higher than the

monofacial system [15]. Finally, there is no a relevant difference among the temperature coefficicients for front and rear side, as studied in [16]. In this paper, a bifacial model based on an electric circuit is proposed. It is based on a previous single-side model. The total solar radiation is calculated in Simulink environment; thus, it can be used also as an input parameter of a PV module into a standard circuit simulator.

2. Model of the PV cell and module

This section is constituted by two parts. The former one derives a mathematical model of a PV cell, starting from the well-known 5-parameters circuit model. The single terms of the descriptive equation are revised, taking into account the Environment Condition (EC). Moreover, the approach is based only on the parameters usually available in the manufacturer's datasheet of a PV module. In this way, the proposed model can be used without a preliminary processing of the information reported in the datasheet. The latter one synthesizes the proposed mathematical model in a lumped electrical circuit, where the solar irradiance is modelled as a variable resistor and the cell temperature as a voltage source. Both of them are evaluated with respect to the Standard Test Conditions (STC) defined later.
Fig. 1 represents the well-known single-diode model of a PV cell [8], whose descriptive equation is:

$$I = I_{Ph} - I_o\left(e^{-\frac{q(V+I\cdot R_S)}{nkT_C}} - 1\right) - \frac{V+I\cdot R_S}{R_{Sh}} \qquad (1)$$

where I_{Ph} [A] is the light generated current (i.e. the short circuit current neglecting the parasitic resistances), I_o [A] is the dark saturation current due to recombination, q [C] is the electron charge, R_s [Ω] is a series resistance, k [J/K] is the Boltzmann's constant, T_c [K] is the solar cell temperature, and R_{sh} [Ω] is a shunt resistance. The 5 unknown parameters are R_s, R_{sh}, n, I_o, I_{ph}.

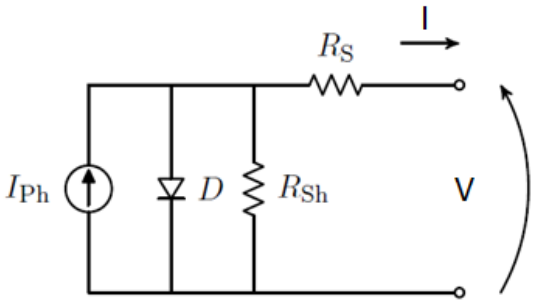

Fig. 1. Single-diode model of a PV cell.

All the parameters are dependent on the EC, primarily the solar radiance G and the air temperature T_a. Thus, (1) can be used after determining the correct value of the parameters R_s, R_{sh}, n, I_o, I_{ph}. in the EC. Moreover, the values of these parameters are not available at all in the datasheet of the PV module, where other specifications are usually shown and are related to the PV module and not to the PV cell: short-circuit current (I_{sc}), open-circuit voltage (V_{oc}), voltage and current in MPP (Vmpp and Impp), rated peak power (P_n), temperature coefficients k_1 and k_2 for I_{sc} and V_{oc}, respectively. All these parameters are defined in STC, i.e. for solar radiation of 1,000W/m^2, air temperature Ta=25°C, air wind of 1 m/s and air mass AM=1.5. Usually, also the Nominal Operating Condition Temperature (NOCT) is defined, but for 800 W/m^2 and cell temperature of 20°C. The NOCT is directly linked to T_a and T_c by the following:

$$T_c = T_a + \frac{G}{800} * (NOCT - 20) \qquad (2)$$

The datasheet contains also information about the number of series- and parallel-connected PV cells in the PV module, therefore it is easy to evaluate the characteristic currents and voltages of a PV cell using the corresponding values of the PV module:

$$V_{cell} = \frac{V_{module}}{n_s} \qquad (3)$$

$$I_{cell} = \frac{I_{module}}{n_p} \qquad (4)$$

being n_s and n_p the number of series- and parallel-connected cells, respectively.
The light generated current is directly proportional to the solar irradiance [17]:

$$I_{Ph} = G_{pu}\cdot[I_{sc}^o + k_1\cdot(T_c - 25)] \qquad (5)$$

where G_{pu}=G⁄1000 is the relative solar irradiance referred to the STC, I_{sc}^o [A] is the short circuit current and the superscript "o" is for STC , k_1 [A/°C] is the current-temperature coefficient at STC, ΔT=(T_c-25) [°C] is the mismatch of the cell temperature with respect to the STC cell temperature.
The structure of (5) is approximately valid also for the Impp:

$$I_{mpp} = G_{pu}\cdot\left[I_{mpp}^o + k_1\cdot(T_c - 25)\right] \qquad (6)$$

The above equation states that the current in MPP depends on both the solar irradiance and the cell temperature.
Let us study the second term of (1). The dark saturation current Io depends on the cell temperature [18], whereas the series resistance Rs depends on the EC [19]. Moreover, it has two characteristic values for V=0 and V=V_{oc}, i.e in short- and open-circuit condition. For these extreme values, it ranges from about zero to I_o. This term can be represented as

$$\beta\cdot e^{\alpha\cdot\frac{T_c}{25}(V+k_2\cdot\Delta T - V_{oc}^o)} \qquad (7)$$

with V_{oc}^o [V] the open circuit voltage at STC, k_2 [V/°C] the voltage-temperature coefficient at STC, α and β the parameters to be calculated, as shown later.
Equation (7) takes into account that the open circuit voltage V_{oc} strongly depends on the cell temperature as [20]:

$$V_{oc} = V_{oc}^{o} - k_2 \cdot \Delta T \quad (8)$$

Also for V_{mpp} is approximately valid the relation:

$$V_{mpp} = V_{mpp}^{o} - k_2 \cdot \Delta T \quad (9)$$

because the values of V_{mpp} and V_{oc} tipically differ less than 15%. For sake of simplicity, we neglect the losses resistances in this paper, thus assuming $R_{sh} \to \infty$. Finally, substituting (5) and (7) into (1), follows (10) that permits to trace the I-V curve in any arbitrary EC. It can be seen that (10) depends on the EC, on the datasheet parameters, and on the α and β parameters.

$$I = G_{pu} \cdot (I_{sc}^{o} + k_1 \cdot \Delta T) - \beta \cdot e^{\alpha \cdot \frac{T_c}{25}(V + k_2 \cdot \Delta T - V_{oc}^{o})} \quad (10)$$

By interpreting the previous equations from a circuital point of view, the circuit of Fig. 2 is carried out.

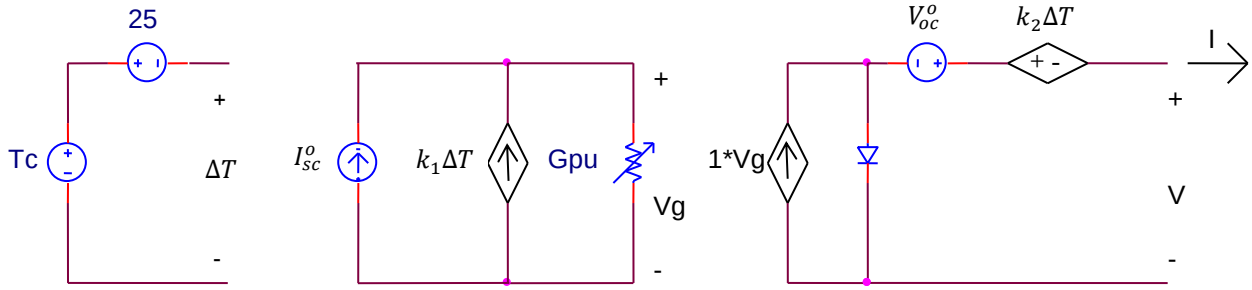

Fig. 2. Electrical circuit of a PV cell, based on eq. (10).

3. Model of the rear solar radiation

The model of Fig. 2 has been derived for a standard mono-facial PV module. Instead, if a bifacial PV module must be implemented, it is needed to consider the front solar radiation and the back one [21]. The authors assumed that the total rear irradiance (I_{Rear}) entering the back of the bifacial solar module is the sum of the direct irradiance ($I_{Rear,dir}$) and diffuse irradiance ($I_{Rear,diff}$) [22,23]. At the rear, it is divided into the amount of irradiance reflected directly from the ground and the amount reflected from the surroundings. The total irradiance is expressed in terms of the GHI (Global Horizontal Irradiance), which is the amount of irradiance incident on the horizontal surface. The total irradiance includes both Direct Normal Irradiance (DNI) and Diffuse Horizontal Irradiance (DHI) [24]. By using the known view factor as element of the back reflection, the irradiance reflected on the rear side of the PV module is determined by the shadow of the module and the outer part of the shadow.
After several mathematical manipulations discussed in [21], it results:

$$I_{Rear} = \alpha DNI \cdot \frac{1 + cos\beta}{2} + \alpha(GHI - DNI) \cdot \left(\frac{1 + cos\beta}{2} - F_m\right)$$

with

$$DNI = 1367 \cdot 23.45° sin\left[\frac{360(d_n + 284)}{365}\right] \cdot 0.7^{AM^{0.678}} \cdot cos\theta_{ZS}$$

where α is the coefficient of albedo due to the rear environment, β is the installation inclination of the module, $\frac{1+cos\beta}{2}$ is a value showing the area where the sunlight is reflected and scattered by the rear environment on the rear part of the module due to the view factor, F_m depends on the view factor, d_n is the number of days that have elapsed since the first day of a year, AM is the Air Mass, θ_{zs} is the angle between the direction perpendicular (Zenith) to the ground and the sun.
Finally, two sub-circuits (as those reported in Fig. 2) have to be considered: one sub-circuit for the radiation of the front side and one sub-circuit for the radiation on the back side; therefore, the two sub-circuits are parallel-connected and the total produced power is due to the sum of the produced currents in the two sub-circuits.
Other researchers proposed a different approach, which consisted in calculating an equivalent single-side radiation G_E that took into account both the front and the rear effects [25]. Therefore, this approach is based on the following equations (considered in STC):

$$G_E = 1000 + \varphi \cdot G_{rear} \quad (11)$$

$$\varphi = \min(\varphi_{Isc}, \varphi_{Pmax}) \quad (12)$$

$$\varphi_{Isc} = \frac{I_{sc,rear}}{I_{sc,front}} \quad (13)$$

$$\varphi_{Pmax} = \frac{P_{max,rear}}{P_{max,front}} \quad (14)$$

where G_{rear} is the rear illumination, φ_{Isc} and φ_{Pmax} are the bifaciality of the shortcircuit current and maximum power, respectively, while $I_{sc,front}$ and $I_{sc,rear}$ are the short-circuit currents.

4. Results

To compare the electrical performances of mono-facial and bifacial PV modules, Figure 3 diagrams the I-V curves of both the mono-facial ($V_{oc} = 32.9V$, $I_{sc} = 8.2A$, $V_{mpp} = 26.3V$, $I_{mpp} = 7.6A$, $P_n = 200W$, $k_1 = 0.0032\ A/K$, $k_2 = -0.123\ V/K$, in STC) and bi-facial PV module. These curves are traced by means of the electrical model of Fig. 2 in STC. Instead, Figure 4 reports the P-V curves, again in the STC, of both the mono-facial and bi-facial module.

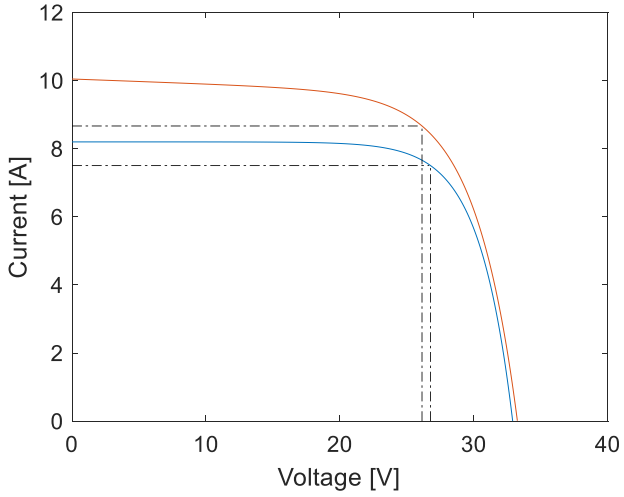

Fig. 3. I-V curve for the mono-facial (blue) and bi-facial (red) PV module in STC.

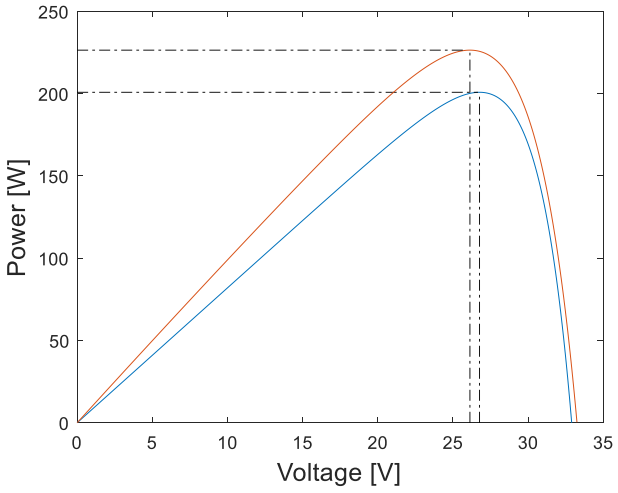

Fig. 4. P-V curve for the mono-facial (blue) and bi-facial (red) PV module in STC.

By comparing the curves in both the Figures 3 and 4, respectively, it results that:

- I_{sc} increases;
- V_{oc} has almost the same value;
- V_{mpp} has a similar value;
- I_{mpp} increases, thanks to the I_{rear};
- P_n increases from 200W to 226W, i.e. an increase of about 13%.

The proposed model is also able to provide the I-V and P-V curves in environmental conditions other than the STC. In fact, Figure 5 diagrams the I-V curve of both the mono-facial and bi-facial PV module, under the solar radiation G=800W/m^2 and the air temperature T_a=20°C. Instead, Figure 6 reports the P-V curves of both the mono-facial and bi-facial module, in the same environmental conditions of Figure 5.

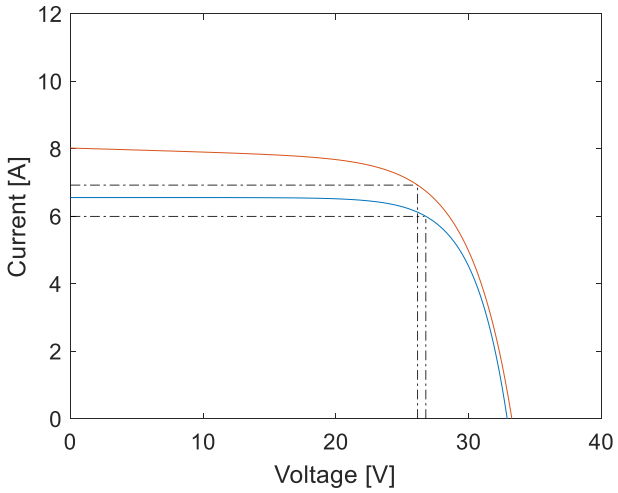

Fig. 5. I-V curve for the mono-facial (blue) and bi-facial (red) PV module, for G=800W/m^2 and T_a=20°C.

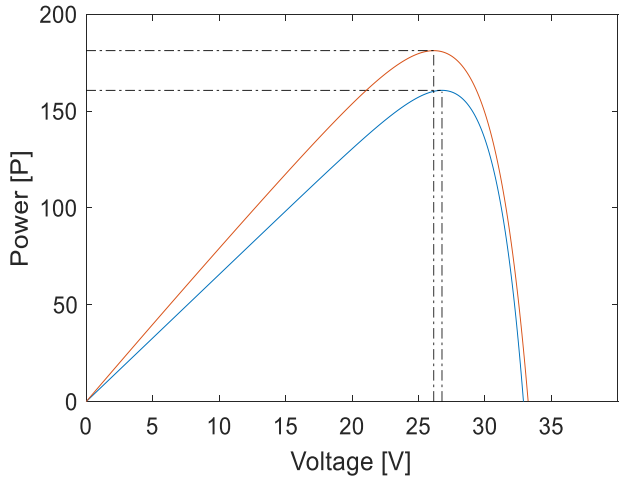

Fig. 6. P-V curve for the mono-facial (blue) and bi-facial (red) PV module, for G=800W/m^2 and T_a=20°C.

5. Conclusions

The paper deals with the modelling of a bifacial PV module. It is based on the model of a mono-facial PV cell in any environment condition and on the model of the rear radiation. As a bifacial module has 2 active surfaces (the front side and the back side), the proposed bifacial model is constituted by two sub-circuits, one for the front side and the other one for the back side. The simulation results confirmed the goodness of the model: in fact, the

bifacial module produces 13% energy more than the mono-facial module and this value is within the range of the gain energy that other researchers have experimentally found, as presented in the Introduction. This technology is very promising, because it allows increasing the power density of the PV plants, i.e. the amount of power produced for square meter of occupied land, which is a very important parameter to consider. Nevertheless, nowadays, several issues are still open, and they can become research opportunities. For example, the effect of the shading on the rear side is not solved, differently from the same issue on the front side. The electronic equipment to acquire separately the electrical variables of both front and rear side is not available. The typical defects of the rear side are not known. The not destructive techniques, usually applied to detect defects on the front side of the PV module (thermography, photo-luminesce, electro-luminescence), cannot be applied in the same way. In summary, most of these issues have been studied for the single-side PV module, by using the mathematical or circuital or thermal model of the PV module. Therefore, also the study of the issues of the double-side PV module can be based on a suitable model, and the proposed model is resulted effective.

References

[1] S. Vergura, Hypothesis tests-based analysis for anomaly detection in photovoltaic systems in the absence of environmental parameters, Energies, 11(3), 485, 2018.

[2] K. J. Sauer, T. Roessler, Systematic Approaches to Ensure Correct Representation of Measured Multi-Irradiance Module Performance in PV System Energy Production Forecasting Software Programs", IEEE Journal of Photovoltaics, 2013, pp. 422–428.

[3] P. Manganiello, M. Ricco, G. Petrone, E. Monmasson, G. Spagnuolo, "Optimization of Perturbative PV MPPT Methods Through Online System Identification", IEEE Trans on INDUSTRIAL Electronics, Vol. 61, Issue 12, 2014, pp. 6812-6821.

[4] S. Vergura, F. Marino, M. Carpentieri, Processing infrared image of PV modules for defects classification, ICRERA 2015, International Conference on Renewable Energy Research and Applications, Palermo, Italy, 2015.

[5] S. Vergura, F. Marino, Quantitative and Computer Aided Thermography-based Diagnostics for PV Devices: Part I – Framework", IEEE Journal of Photovoltaics, Vol. 7, Issue 3, May 2017, pp 822-827.

[6] S. Vergura, M. Colaprico, M. F. de Ruvo, F. Marino, "A Quantitative and Computer Aided Thermography-based Diagnostics for PV Devices: Part II – Platform and Results", IEEE Journal of Photovoltaics, Vol. 7, Issue 1, January 2017, pp 237-243.

[7] S. Vergura, E. Natangelo, Labview-matlab integration for analyzing energy data of PV plants, RE&PQJ (ISSN 2172-038X), Renewable Energy & Power Quality Journal, No.8, 635, April 2010.

[8] Y. Mahmoud, W. Xiao, and H. H. Zeineldin, "A Parameterization Approach for Enhancing PV Model Accuracy," IEEE Transactions on Industrial Electronics, vol. 60, no. 12, pp. 5708 - 5716, Dec. 2013.

[9] S. Vergura, A. Massi Pavan, "On the photovoltaic explicit empirical model: Operations along the current-voltage curve", IEEE-ICCEP 2015, International Conference on Clean Electrical Power, Taormina, Italy, June 16–18, 2015, pp. 99-104.

[10] V. Lo Brano, A. Orioli, G. Ciulla, and A. Di Gangi, An Improved Five-Parameter Model for Photovoltaic Modules. Solar Energy Materials & Solar Cells, 94, pp.1358-1370, 2010.

[11] A. Massi Pavan, S. Vergura, A. Mellit, V. Lughi, Explicit empirical model for photovoltaic devices. Experimental validation, Solar Energy, Vol. 155, October 2017, pp. 647-653.

[12] C. Deline *et al.*, "Assessment of Bifacial Photovoltaic Module Power Rating Methodologies—Inside and Out", IEEE Journal of Photovoltaics, Vol. 7, Issue 2, March 2017, pp 575-580.

[13] U. A. Yusufoglu *et al.*, "Analysis of the annual performance of bifacial modules and optimization methods", IEEE Journal of Photovoltaics, Vol. 5, Issue 1, January 2015, pp 320-328.

[14] S. A. Pelaez, C. Deline, S. R. MacAlpine, B. Marion, J. S. Stein, R. K. Kostuk, "Comparison of Bifacial Solar Irradiance Model Predictions With Field Validation", IEEE Journal of Photovoltaics, Vol. 9, Issue 1, January 2019, pp 82-88.

[15] S. A. Pelaez, C. Deline, P. Greenberg, J. S. Stein, R. K. Kostuk, "Model and Validation of Single-Axis Tracking With Bifacial PV", IEEE Journal of Photovoltaics, Vol. 9, Issue 3, May 2019, pp 715-721.

[16] J. Lopez-Garcia, D. Pavanello, T. Sample, "Analysis of Temperature Coefficients of Bifacial Crystalline Silicon PV Modules", IEEE Journal of Photovoltaics, Vol. 8, Issue 4, July 2018, pp 960-968.

[17] Townsend, T. U., M.S. Thesis, Mechanical Engineering, U. of Wisconsin Madison, "A Method for Estimating the Long-Term Performance of Direct-Coupled Photovoltaic Systems", 1989.

[18] Priyanka Singh, N.M. Ravindra, "Temperature dependance of solar cell performance – an analysis", Solar Energy Materials and Solar Cells, vol. 101, pp. 36-45, 2012.

[19] T. Markvart, L. Castaner. Practical Handbook of Photovoltaics. Fundamentals and applications. Oxford, UK, 2006.

[20] A. Luque, S. Hegedus. Handbook of photovoltaic science and engineering. Chichester, UK, 2003.

[21] Cha, H.L., Bhang, B.G., Park, S.Y., Choi, J.H., Ahn, H.K., Power prediction of bifacial Si PV module with different reflection conditions on rooftop, Applied Sciences, Vol. 8, Issue 10, September 2018.

[22] SolarWorld. How to Maximize Energy Yield with Bifacial Technology. White Paper. 2016. online: https://solarkingmi.com/assets/How-to-Maximize-Energy-Yield-with-Bifacial-Solar-TechnologySW9001US.pdf.

[23] Hansen, C.W.; Stein, J.S.; Deline, C.; MacAlpine, S.; Marion, B.; Asgharzadeh, A. Analysis of irradiance models for bifacial PV modules. In Proceedings of the IEEE 43rd Photovoltaic Specialists Conference (PVSC, Portland, USA, 5–10 June 2016, pp. 138–143.

[24] Yusufoglu, U.A.; Lee, T.H.; Pletzer, T.M.; Halm, A.; Koduveliklathu, L.J.; Comparotto, C.; Kurz, H. Simulation of energy production by bifacial modules with revision of ground reflection. Energy Procedia 2014, 55, 389–395.

[25] Y. Zhang, Q. Gao, Y. Yu, Z. Liu, "Comparison of Double-Side and Equivalent Single-Side Illumination Methods for Measuring the I–V Characteristics of Bifacial Photovoltaic Devices", IEEE Journal of Photovoltaics, Vol. 8, Issue 2, March 2018, pp 397-403.